

Discovery of Vanoxerine Dihydrochloride as a CDK2/4/6 Triple-Inhibitor for the Treatment of Human Hepatocellular Carcinoma

Ying Zhu

Kunming Medical University

Xi-Nan Shi

yunnan university of chinese medicine

Zhong-Kun Xia

Zhengzhou University

Hong-Jian Li

Chinese University of Hong Kong

Rong Su

Kunming Medical University

Kun-Bin Ke

Kunming Medical University

Chao Dong

Kunming Medical University

Feng-Mei Zhou

Zhengzhou University

Lin Wang

Zhengzhou University

Rong Chen

Yunnan university of chinese medicine

Shi-Guo Wu

yunnan university of chinese medicine

Hui Zhao

Kunming Medical University

Peng Gu

Kunming Medical University

Kwong-Sak Leung

Chinese University of Hong Kong

Man-Hon Wong

Chinese University of Hong Kong

Gang Lu

Chinese University of Hong Kong

Jian-Ying Zhang

Zhengzhou University

Bing-Hua Jiang

Zhengzhou University

Jian-Ge Qiu (✉ jiangeqiu@zzu.edu.cn)

Zhengzhou University <https://orcid.org/0000-0003-3885-0775>

Marie Chia-mi Lin

Zhengzhou University

Research article

Keywords: Cyclin-dependent kinases 2/4/6, hepatocellular carcinoma, vanoxerine dihydrochloride, triple inhibitor, drug combination

Posted Date: May 27th, 2020

DOI: <https://doi.org/10.21203/rs.3.rs-29276/v1>

License:   This work is licensed under a Creative Commons Attribution 4.0 International License. [Read Full License](#)

Version of Record: A version of this preprint was published on February 12th, 2021. See the published version at <https://doi.org/10.1186/s10020-021-00269-4>.

Abstract

Background Cyclin-dependent kinases 2/4/6 (CDK2/4/6) play critical roles in cell cycle progression, and their deregulations are hallmarks of hepatocellular carcinoma (HCC).

Methods Here we combined computational and experimental approaches to discover a CDK2/4/6 triple-inhibitor from FDA approved small-molecule drugs for the treatment of HCC.

Results Based on molecular docking results, vanoxerine dihydrochloride was found to exhibit strongest cytotoxic effect on human HCC QGY7703 and Huh7 cells (IC₅₀: 3.79 μM for QGY7703 and 4.04 μM for Huh7 cells). Vanoxerine dihydrochloride treatment caused G1 arrest, induced apoptosis, and reduced the expressions of CDK2/4/6, cyclin D/E, retinoblastoma protein (Rb), as well as the phosphorylation of CDK2/4/6 and Rb in QGY7703 and Huh7 cells. In addition, combined vanoxerine dihydrochloride and 5-Fu produced synergistic cytotoxicity in Huh7 cells. Finally, *in vivo* studies in preclinical animal model of BALB/C mice subcutaneously xenografted with Huh7 cells, we showed that injection of vanoxerine dihydrochloride (40 mg/kg, i.p.) produced significant antitumor activity ($p < 0.05$), comparable to that achieved by 5-Fu (10 mg/kg, i.p.), with the combination treatment resulted in strongest effect.

Conclusions The present study is the first to identify a CDK2/4/6 triple inhibitor vanoxerine dihydrochloride, and demonstrate that it represents a novel therapeutic strategy for HCC treatment alone or in combination with 5-Fu.

Introduction

Hepatocellular carcinoma (HCC), the most common type of liver cancer, is the second[1] cause of cancer-related death world wide. Surgical resection is the first line treatment, followed by liver transplantation and percutaneous ablation. However, there is a high frequency of tumor recurrence after surgical resection. Unfortunately, most HCCs are resistant to conventional chemotherapy and radiotherapy[2]. Emerging targeted therapies have provided new treatment options[3], with sorafenib, a multitarget tyrosine kinase inhibitor (TKI) approved by FDA for the treatment of unresectable HCC. However, rapid development of drug resistance limited the uses. There is urgent need for the development of more drugs targeting different mechanisms.

Cyclin-dependent kinases (CDKs) are important targets for cancer therapy, as they play critical roles in cell cycle and cell growth/differentiations[4, 5]. There are two categories of CDKs. The first one, includes CDK1, CDK2, CDK4 and CDK6, regulates cell cycle progression from G0 phase to G1, and S phases[6, 7]. The second one, such as CDK7-11 and CDK14-20, regulate gene transcription[8, 9] and Wnt signaling[10]. Drugs that inhibiting various CDKs have long been evaluated as cancer therapeutics[5, 11–13]. Currently, the third generation CDK4/6 dual inhibitors palbociclib, ribociclib, and abemaciclib have been approved by FDA for the treatment of breast cancer[14]. Unfortunately, they have only limited benefits for the treatment of HCC or other cancers, suggesting the need for the development of more effective CDK inhibitors.

It has been demonstrated that the dysregulation of any one of the CDK2/4/6 is sufficient to cause HCC. For example, transgenic mice overexpressing either CDK2 or CDK4 or CDK6, all led to the development of liver cancer[15]. Furthermore, significantly elevated expressions of CDK2, CDK4, and CDK6 are well documented in

many cancers including HCC[16–19], and they are the causal factors for the development and progression of cancer. Therefore, a CDK2/4/6 triple-inhibitor appears to be a logical strategy for the treatment of HCC.

We have previously reported the identification of two CDK2 inhibitors, Adapaline and Fluspirilene and one CDK4/6 dual inhibitor Rafoxanide[20–22]by the combination of computer-aided strategies and the experimental validations. In this study, we extended these strategies to screen for CDK2/4/6 triple inhibitors from FDA approved drugs, and discovered vanoxerine dihydrochloride as a new CDK2/4/6 triple inhibitor for the treatment of HCC. Vanoxerine dihydrochloride exhibited strong cytotoxic effect in human HCC QGY7703 and Huh7 cells. It caused G1arrest, induced apoptosis, and reduced the expressions of CDK2/4/6, cyclin D/E, retinoblastoma protein (Rb). We also validated its efficacy *in vivo* in BALB/C nude mice xenografted subcutaneously with Huh7 cells. The antitumor activity of vanoxerine dihydrochloride was comparable to that achieved by 5-Fu. Furthermore, combined administration of vanoxerine dihydrochloride and 5-Fuproduced synergistic effect.

To our knowledge, this is the first report identifying a CDK2/4/6 triple inhibitor. As a FDA approved drug, the potential use of vanoxerine dihydrochloride for the treatment of HCC warrants further investigations.

Materials And Methods

Ethics statement

The animal studies were approved by the Kunming Medical University's laboratory animal ethics committee.

Docking

The X-ray crystallographic structures used in the studies were obtained from the Protein Data Bank (PDB)[23, 24]. In addition to 5 structures of CDK4 and 8 structures of CDK6, we also collected 14 structures of CDK2. The chemical structures of a total of 3167 US Food and Drug Administration (FDA) approved drugs were gathered from the ZINC database.[25, 26]. We used the docking software idock v2.2.1[27, 28] to dock all of the compounds onto the CDK4/6 structures first. The binding conformations and the binding affinities were predicted and prioritized according to the average predicted binding affinity. Then the top 50 ranking candidate CDK4/6 inhibitors were docked onto the CDK2 structures to screen for CDK2/4/6 triple inhibitors. Nine top ranking commercially available compounds were selected and evaluated.

Chemicals.

Monatepil, Fluazuron, Temafloxacin, Ketanserin, Talniflumate, Altanserin, Dutasteride, Mizolastine, Vanoxerine dihydrochloride, 5-Fu were purchased from Sigma-Aldrich.

Cell lines, cell culture, and experimental conditions.

The human HCC cell lines QGY7703 and Huh7 were obtained from Cell bank of Chinese Academy of Sciences (Shanghai, China), and cultured in D-MEM/F-12 medium (GIBCO, USA) containing 8% FBS (Hyclone, Mexico) at 37°C in 5% CO₂ and 95% humidified air. Cells were plated in 96-, 24-plates (NEST, China) with medium containing 8% FBS and the test compounds at indicated concentrations (1, 3, 10 and 30 μM), and then incubated for indicated times (6, 12, 24, 48 or 72 h).

Cell viability MTT and CCK-8 assays.

MTT assay were conducted as described in previous studies[20-22]. QGY7703 and Huh7 cells were plated at an initial density of 9×10^3 cells/well in 96-well plates, incubated with MTT (Sigma) reagents and the absorbance measured at 570 nm with a microplate reader (Multiskan Spectrum, Thermo Scientific *Microplate Reader*, USA). CCK-8 assay was performed as described in the CCK-8 Kit (Dojindo Laboratories). Cells were seeded in 96-well plate, treated with various drugs for indicated time prior to the addition of CCK-8 solution and OD values were measured at 450 nm using a microplate reader.

Cell cycle analysis.

The cell cycle profile was determined by Flow cytometry analysis, as described previously[20-22]. Briefly, QGY7703 and Huh7 cells (4×10^4) were seeded in 24-well plates in D-MEM/F-12 medium. After 24 h culture, medium were replaced with D-MEM/F-12 containing 8% FBS and vanoxerine dihydrochloride (1, 3, 10 or 30 μM) for indicated times (6, 12 or 24 h), fixed in ice-cold ethanol, and stained in Coulter DNA-Prep Reagents (Beyotime Coulter, Beyotime Institute of Biotechnology, Beijing). The cellular DNA content was determined by EPICS xL4 flow cytometer (BD FACSCalibu, USA), and cell cycle distribution determined by BD FACStation software (USA).

Cell apoptosis

QGY7703 and Huh7 cells were seeded in 6-well plate in D-MEM/F-12 medium. After 48 hours culture, the medium were replaced with D-MEM/F-12 containing 8% FBS and vanoxerine dihydrochloride (1, 3, 10 or 30 μM) for indicated times (6, 12 or 24 h). Apoptosis was measured by annexin V and propidium iodide (PI) staining (Beyotime Institute of Biotechnology, Beijing) as described in previous studies[20-22].

Western blot analysis.

Cells were lysed and Western blotting analysis were performed as described previously[20-22]. QGY7703 and Huh7 cells were plated at 6-well plates, cultured in serum starved media (0.125% FBS) for 24 hours and then with 10% FBS medium containing various concentrations (3, 10, 30 μM) of vanoxerine dihydrochloride. Cells were harvested after 6 hours incubation and proteins analyzed by Western blotting. Primary antibodies were purchased from Cell Signaling Technology, Inc. Danvers, MA, USA). They include anti-cyclin D1 (no. 2978), anti-cyclin E (no. 4129), anti-CDK2/4/6 (no. 2546), anti-Rb (no. 9313), anti-phospho-CDK4,

anti-phospho-CDK2/4/6 (no. 2561), anti-Rb (no. 9301), and anti-GAPDH (no. 5174). As positive controls, three siRNAs targeting each of the CDK2/4/6 were designed as described previously [22], and used to inhibit the expressions of each of the CDK2/4/6 proteins in QGY7703 and Huh7 cells. The proteins were measured using enhanced chemiluminescence detection system (Thermo Fisher scientific, USA).

Synergy quantitation of the combination treatment

Synergy quantitation of the drug combination studies were performed according to the Chou–Talalay method. Huh7 cells were plated at an initial density of 5×10^3 cells/well in 96-well plates, and treated cells with various concentrations of vanoxerine dihydrochloride and 5-Fu. Cell viability was detected by CCK-8 after 72 hours treatment, and the absorbance values were measured at 450 nm using microplate reader. The combined effect was analyzed by CompuSyn software (www.combosyn.com), which performs multiple drug dose-effect calculations using the Median Effects methods described by Chou and Talalay to determine the combination index (CI). The drug combinations quantitative definition of CI for additive effect (CI = 1), for synergism is CI < 1, and for antagonism is CI > 1. (The formula of the combined index of the two drugs is: $CI = (D_1)/(Dx_1) + (D_2)/(Dx_2)$, Single dose (D), combined dose (Dx)) [29].

Determine the anti-cancer efficacy in nude mice xenografted with Huh7 cancer cells.

Female BALB/C nude mice (4-5 weeks old, weighing 15 g; Animals laboratory of Kunming Medical University China), were housed and cared under standard conditions (pathogen-free, 12 h light/dark cycle, 50-80% humidity, and 15-27°C) in accordance with guidelines from animal ethics committee in Kunming Medical University. For the preclinical animal model, Huh7 cells (1×10^6 cells in 0.2 ml PBS) were subcutaneously injected into the right flank of the nude mice. The size of the tumor was measured every day by a caliper, and tumor volume calculated by the formula $V = ab^2/2$ (a=longest axis; b=shortest axis). When the tumors grew to 80-100 mm^3 (7 days after inoculation), mice were divided randomly into 4 groups (5 mice/group), and treated for 21 days by i.p. injection daily of (1) control PBS, (2) vanoxerine dihydrochloride (40mg/kg), (3) 5-Fu (10mg/kg), (4) vanoxerine dihydrochloride (40mg/kg) plus 5-Fu (10mg/kg). At the end of experiments, mice were sacrificed by cervical dislocation. The tumor tissues were excised, weighed, images captured, and immunohistochemistry analysis performed.

Immunohistochemistry

Tumor tissues were fixed in 10% formalin and embedded in paraffin, sliced into 4 μm sections, deparaffinized, dehydrated, antigen retrieved, blocked with 5% goat serum, and incubated in the primary antibodies: anti-RB1 (1: 500; CST), anti-CDK2 (1:50; Abcam), anti-CDK4 (1: 500; CST), anti-CDK6 (1: 100 Abcam). The slides were washed and incubated with biotinylated anti-mouse or anti-rabbit secondary antibodies. The peroxidase reaction was visualized using 3,3'-diaminobenzidine tetrahydrochloride (DAB) and counterstained with hematoxylin. To quantitate the staining intensity, 5 random fields were chosen, and the numbers of total cells

and positive cells were counted in each section under a microscope at 400x magnification. The percentage of positive cell populations from the 5 random fields was analyzed for statistics.

Statistical Analysis.

Data were obtained from the triplicates of three different experiments. Values are expressed as the mean \pm standard deviation. The data were analyzed by SPSS software (version 16.0). $P < 0.05$ was considered to indicate statistically significant difference between values.

Results

Discovery of CDK2/4/6 triple-inhibitors via computer-aided structure-based virtual screening

The chemical structures of a total of 3167 US Food and Drug Administration (FDA) approved drugs were gathered from the ZINC database, docked onto the CDK4 and CDK6 structures, and then sorted in the ascending order of their predicted binding free energy. Then, the top 50 ranking candidate CDK4/6 inhibitors were docked onto CDK2 structures to screen for CDK2/4/6 triple inhibitors. We manually examined the high-scoring compounds based on *in silico* estimations of binding strength, appropriate molecular weight and other drug-like properties, and complementary matching of molecular shape. The highest-scoring compounds were identified and nine commercially available compounds (Table 1) were selected for subsequent validations[30–38]

Table 1
The nineteen top-scoring compounds purchased and tested in vitro

compounds name	ZINC ID	average idock score(kcal/mol)	MW(g/Mol)	clinic usage	Ref.
Monatepil	1851142	-9.57	475.62	Ca ²⁺ + channel antagonist	[30]
Fluazuron	2570819	-10.05	506.21	insecticides	[31]
Temafloxacin	9133461	-9.58	417.38	difluoro quinolone antimicrobial agent	[32]
Ketanserin	537877	-9.36	545.51	a selective 5-HT ₂ receptor antagonist	[33]
Talniflumate	1844627	-10.08	414.33	inhibitor of human calcium-activated chloride channels	[34]
Altanserin	26174383	-9.58	411.49	The selective 5-hydroxytryptamine ₂ (5-HT ₂) receptor antagonist	[35]
Dutasteride	3932831	-9.58	528.53	Selective inhibition of type 2 5 α -reductase	[36]
Mizolastine	13831810	-9.48	432.49	selective H ₁ -receptor blocker	[37]
Vanoxerine dihydrochloride	22034135	-8.83	523.49	inhibitor of uptake of dopamine and norepinephrine	[38]
An idock score is the estimated binding free energy (kcal/mol units). Negative value implies a high predicted binding affinity.					

The cytotoxicity of candidate drugs on human HCC QGY7703 and Huh7 cells.

We first evaluated the effects of these nine compounds (monatepil, fluazuron, temafloxacin, KETANSERIN, talniflumate, altanserin, dutasteride, mizolastine, vanoxerine dihydrochloride) on reducing the cell viability, as determined by MTT assay. These compounds caused reduced cell viability on QGY7703 (Fig. 1A) and Huh7 cells (Fig. 1B), with vanoxerine dihydrochloride most effective in both cell lines. Furthermore, the inhibitory effect of vanoxerine dihydrochloride was dose and time dependent (Fig. 1C, 1D), with the IC₅₀ values calculated using GraphPad Prism5 to be 3.79 μ M for QGY7703 and 4.04 μ M for Huh7 cells.

Vanoxerine dihydrochloride treatment caused cell cycle arrest and apoptosis in QGY7703 and Huh7 cells.

To demonstrate that vanoxerine dihydrochloride is a CDK2/4/6 triple inhibitor, we treated QGY7703 and Huh7 cells with vanoxerine dihydrochloride (3, 10 or 30 μ M) for 6, 12 or 24 h, and determined its effects on the cell cycle profiles, using flow cytometry analysis. As shown in Fig. 2, vanoxerine dihydrochloride treatment significantly ($p < 0.05$) caused the G₁ phase arrest in a dose and time dependent manner in QGY7703 (Fig. 2A) and Huh7 (Fig. 2B) cells. Significantly decreased cell populations in the S-phase and G₂-M phase were also

observed in QGY7703 (Fig. 2C) and Huh7 (Fig. 2D) cells at 24 h after treatment. In addition, we also showed that vanoxerine dihydrochloride treatment significantly promoted cell apoptosis, as determined by flowcytometry analysis using the annexinV and propidium iodide staining. Vanoxerine dihydrochloride treatment (at 3, 10, 30 μ M for 6, 12, 24 h) significantly increased the percentage of apoptotic cells in a dose- and time-dependent manner in QGY7703 (Fig. 3A) and Huh7 (Fig. 3B) cells.

Vanoxerine dihydrochloride decreased the expressions and phosphorylations of CDK2/4/6.

Western blotting analysis was used to measure the effects of vanoxerine dihydrochloride treatment on the expressions and phosphorylations of CDK2/4/6, downstream target protein Rb, and their binding partners cyclinD/E, in QGY7703 and Huh7 cells. As expected of CDK2/4/6 triple inhibitor, vanoxerine dihydrochloride significantly and dose-dependently decreased the expressions of CDK2/4/6, the phosphoCDK2/4/6, the binding partners cyclinE and cyclinD, as well as the down-stream target proteins Rb and phosphoRb in QGY7703 (Fig. 4A, 4C) and Huh7 (Fig. 4B, 4D) cells. In summary, we proposed the molecular mechanisms of vanoxerine dihydrochloride (Fig. 5), in which vanoxerine dihydrochloride inhibited CDK4/6 phosphorylation, which reduced the complex of cyclinD and CDK4/6. As a CDK2 inhibitor, it also inhibited CDK2 phosphorylation, which reduced the complex of cyclinE-CDK2. Together, they caused the subsequent reduction of Rb phosphorylation as well as the activation of E2F, to inhibit G1-S transition and produce G1 arrest. In addition, it is also expected to suppress the activation of cyclinA-CDK2 complex to decrease DNA replication and cell cycle S to G2-M phase transitions, which is consistent with what we observed from the cell cycle profiles analysis.

The predicted conformations of vanoxerine dihydrochloride and CDK2/4/6.

The predicted two-dimensional chemical structure of vanoxerine dihydrochloride is shown in Fig. 6A. Based on the results from computer docking, we predicted that vanoxerine dihydrochloride interacts with CDK2 and resides in the ATP-binding site of CDK2 with hydrophobic binding with ILE10, LYS33, VAL64, PHE80, ALA144, and a salt bridge with ASP145, and a halogen bond with GLU81 (Fig. 6B). It interacts with CDK4 ATP-binding site through two salt bridges with ASP104, a π interaction with LYS40, and a halogen bond with PHE98 (Fig. 6C), and interacts with CDK6 ATP binding site through a hydrogen bond with ILE19, a salt bridge with ASP104 and a π interaction with PHE98 (Fig. 6D). Results from western blotting indicated that vanoxerine dihydrochloride inhibited the activities of CDK2/4/6 with similar efficacy, suggesting that it has comparable binding affinity to all three CDKs.

Vanoxerine dihydrochloride and 5-FU produced synergistic cytotoxic effects in vitro in Huh7 cells.

To test the potential synergistic effect of combination therapy, Huh7 cells were seeded in 96-well plates and treated with combinations of various concentrations of vanoxerine dihydrochloride (3 μ M, 10 μ M, 30 μ M) and 5-Fu (1 μ M, 3 μ M, 10 μ M, 30 μ M, 100 μ M). Cell viability was detected by CCK8 assay 72 hours after treatment (Fig. 7A-7B). The drug combination effect and the combination index (CI) were analyzed by CompuSyn software to calculate the multiple drug dose-effect using the Median Effects methods described by Chou and Talalay. The quantitative definition of drug combinations for additive effect is (CI = 1), synergism is (CI < 1), and antagonism is (CI > 1). Vanoxerine hydrochloride 10 μ M, and 5-Fu 1 μ M, 3 μ M, 30 μ M, 100 μ M, all showed

combined synergistic effect(CI \leq 1). CI were also used in the combined action point diagram (Fig. 7C) to quantitatively describe the synergism and antagonism of combined drugs at a given dose-effect level.

Vanoxerine dihydrochloride administration reduced the growth of xenografted Huh7 tumors in vivo in nude mice.

Huh7 cells (1×10^6 cells in 0.2 ml PBS) were subcutaneously injected into the right flank of BALB/C nude mice. When the tumors grew to 80–100 mm^3 (7 days after inoculation), mice were divided randomly into 4 groups (5 mice/group), and treated daily for 21 days by i.p. injection of (1) control PBS, (2) vanoxerine dihydrochloride (40 mg/kg), (3) 5-Fu (10 mg/kg), (4) vanoxerine dihydrochloride (40 mg/kg) plus 5-Fu (10 mg/kg), and the tumor volume and body weight were recorded. At the end of experiments, mice were sacrificed by cervical dislocation. The tumor tissues were excised, weighed, images captured (supplement Fig. 3), and immunohistochemistry analysis performed. Vanoxerine dihydrochloride and 5-FU treatments both significantly reduced tumor weight (Fig. 8A) and tumor volume (Fig. 8B), with comparable efficacy, and the combination of vanoxerine dihydrochloride and 5-FU produced the strongest therapeutic effect. As shown in Fig. 8C, all treatments had no obvious effect on body weight. Immunohistochemistry staining of the tumor tissues showed significantly reduced expressions of Rb (Fig. 8D), CDK2 (Fig. 8E), CDK4 (Fig. 8F), and CDK6 (Fig. 8G) in vanoxerine dihydrochloride treatment group, as compared to control PBS treatment group. In contrast, 5-Fu did not show significant effect. Furthermore, the combination of vanoxerine dihydrochloride and 5-FU appeared to further decrease the expressions of these proteins.

Discussions

In recent years, a large number of CDK inhibitors have been reported. The first generation inhibitors flavopiridol, (R)-roscovitine, and olomoucine, had low individual CDK specificity, low therapeutic efficacy and high toxicity[39, 40]. The second generation of CDK inhibitors including dinaciclib, AT7519, milciclib, TG02, CYC065 and RGB-286638 demonstrated little clinical activity[41–45]. In 2015, a selective CDK 4/6 inhibitor palbociclib was approved by FDA as the first CDK inhibitor the treatment of breast cancer[15]. However, so far, no CDK inhibitor has been approved for the treatment of HCC or other cancers, suggesting the need to find more effective drugs, and a CDK2/4/6 triple inhibitor may be a potential candidate.

In this study, we used computer-aided strategy to screen for CDK2/4/6 triple inhibitors, and successfully discovered vanoxerine dihydrochloride. We propose that a CDK2/4/6 triple-inhibitor may offer some advantages over CDK4/6 dual-inhibitor in providing broader patient selection, higher efficacy, and broader types of cancers for treatment.

Firstly, CDK2, CDK4, and CDK6, these three CDKs are often all elevated in clinical patient samples of many cancers. In HCC, CDK2, CDK4, and CDK6 have been shown to be elevated in 84%[16], 66.7%[17], and 46%[18] of clinical patient samples, respectively. In lung cancers, CDK2 levels were over-expressed in more than 90% [46], and CDK4/6 in more than 23% of the patient samples[47, 48] Therefore, a CDK 2/4/6 triple inhibitor will likely be more effective than CDK4/6 dual inhibitor in these cancers.

In addition, CDK2 has different and broader functions than CDK4/6. The CDK4/6 promote cell cycle G1-S phase transition through activate cyclinD-CDK4/6 complexes[5, 49], hyper-phosphorylate Rb on serine and threonine residues.[50], and stimulate the release of E2F transcription factor, which facilitates the transcription of genes required for G1toS transition and Sphase progression. CDK2 works differently. It promotes G1-S phase transition through activation of cyclin E-CDK2 to maintain Rb phosphorylation. It also activates cyclinA-CDK2 complexes, to initiate DNA synthesis and the S phase cell cycle. In addition, CDK2 has been reported to phosphorylate the p27^{KIP1} and RB proteins in cell cycle progression, the replication factors A and C in DNA replication, the NPAT in histone synthesis, and the nucleophosmin (NPM) in centrosome duplication[51]. Therefore, as a CDK2/4/6 triple inhibitor, vanoxerine dihydrochloride will likely to have broader anti-cancer activities in addition to the CDK4/6–RB axis.

Furthermore, we demonstrated the synergic effect of combining vanoxerine dihydrochloride with chemotherapy drug 5-Fu both *in vitro* in cell lines and *in vivo* in preclinical animal models. The combination therapies have already been shown to be beneficial for CDK4/6 dual inhibitors. For examples, FDA has approved the use of palbociclib in combination with fulvestrant for the treatment of hormone receptor-positive, HER2-negative metastatic breast cancer[52]. The potential additive or synergistic effect of combination therapy of vanoxerine dihydrochloride with other targeted therapies, chemotherapies, radiotherapy or immunotherapies warrant further investigations.

At present, vanoxerine dihydrochloride is mainly used as dopamine uptake inhibitor[53–56], as it inhibits the re-uptake of dopamine and norepinephrine. Vanoxerine dihydrochloride is relatively safe for human use. The adverse effects reported in human patients included dopaminergic effects and arrhythmia[57]. In preclinical studies in mice, the reported LD50 (oral) is 500 mg/kg[38, 57], and no obvious toxic effects were reported following either intraperitoneal (i.p.) injection at 20 mg/kg, or oral administration at 20 mg/kg[57]. Consistently, in the present study we did not observe any significant changes in the body weight of the BALB/C nude mice administered (i.p.) with vanoxerine dihydrochloride (40 mg/kg) over 21 days, suggesting that it is a relatively safe drug for cancer treatment.

To the best of our knowledge, the present study was the first to report that vanoxerine dihydrochloride is a CDK2/4/6 triple inhibitor, and that vanoxerine dihydrochloride exhibited significant *in vivo* anticancer efficacy. As a FDA approved drug, the use of vanoxerine dihydrochloride for the treatment of HCC and other cancers warrant further investigations.

Declarations

Acknowledgements

Not applicable.

Funding

The present study was supported by the Yunnan Applied Basic Res of Combined Foundation of Yunnan Province Science & Technology Dept. and Kunming Medical University (2017FE467(-186), 2018FE001(-069), 2019FE001-064), Yunnan Applied Basic Res. of Combined Foundation of Yunnan Province Science &

Technology Dept , Yunnan Univ. of Chinese Medicine (2018FF001(-026), 2019FF002(-050,-040)), GuiZhou Science & Technology Department [NO. QKHJC (2017)1171], Top young talents of ten thousand talents plan in Yunnan Province (2019), the Scientific Research Foundation of Yunnan Education Department (2018JS208, 2018JS226), and General Research Projects in Yunnan Province (2019FB113), the National Natural Science Foundation of China (No.81803197, No.81903174).

Consent for publication

Not applicable.

Competing interests

The authors declare that they have no competing interests.

References

1. Mazzanti R, Arena U, Tassi R. Hepatocellular carcinoma: Where are we? *World journal of experimental medicine*. 2016;6(1):21–36.
2. Llovet JM, Villanueva A, Lachenmayer A, Finn RS. Advances in targeted therapies for hepatocellular carcinoma in the genomic era. *Nature reviews Clinical oncology*. 2015;12(7):408–24.
3. Jindal A, Thadi A, Shailubhai K. Hepatocellular Carcinoma: Etiology and Current and Future Drugs. *Journal of clinical experimental hepatology*. 2019;9(2):221–32.
4. Lim S, Kaldis P. Cdks, cyclins and CKIs: roles beyond cell cycle regulation. *Development*. 2013;140(15):3079–93.
5. Asghar U, Witkiewicz AK, Turner NC, Knudsen ES. The history and future of targeting cyclin-dependent kinases in cancer therapy. *Nature reviews Drug discovery*. 2015;14(2):130–46.
6. Hinz M, Krappmann D, Eichten A, Heder A, Scheidereit C, Strauss M. NF-kappaB function in growth control: regulation of cyclin D1 expression and G0/G1-to-S-phase transition. *Molecular cellular biology*. 1999;19(4):2690–8.
7. Lukas J, Bartkova J, Bartek J. Convergence of mitogenic signalling cascades from diverse classes of receptors at the cyclin D-cyclin-dependent kinase-pRb-controlled G1 checkpoint. *Molecular cellular biology*. 1996;16(12):6917–25.
8. Peng J, Marshall NF, Price DH. Identification of a cyclin subunit required for the function of Drosophila P-TEFb. *J Biol Chem*. 1998;273(22):13855–60.
9. Nemet J, Jelacic B, Rubelj I, Sopta M. The two faces of Cdk8, a positive/negative regulator of transcription. *Biochimie*. 2014;97:22–7.
10. Sun T, Co NN, Wong N. PFTK1 interacts with cyclin Y to activate non-canonical Wnt signaling in hepatocellular carcinoma. *Biochem Biophys Res Commun*. 2014;449(1):163–8.
11. Canavese M, Santo L, Raje N. Cyclin dependent kinases in cancer: potential for therapeutic intervention. *Cancer Biol Ther*. 2012;13(7):451–7.

12. Peyressatre M, Prevel C, Pellerano M, Morris MC. Targeting cyclin-dependent kinases in human cancers: from small molecules to Peptide inhibitors. *Cancers*. 2015;7(1):179–237.
13. Shen S, Dean DC, Yu Z, Duan Z. Role of cyclin-dependent kinases (CDKs) in hepatocellular carcinoma: Therapeutic potential of targeting the CDK signaling pathway. *Hepatology research: the official journal of the Japan Society of Hepatology*. 2019;49(10):1097–108.
14. Spring LM, Wander SA, Zangardi M, Bardia A. CDK 4/6 Inhibitors in Breast Cancer: Current Controversies and Future Directions. *Current oncology reports*. 2019;21(3):25.
15. Otto T, Sicinski P. Cell cycle proteins as promising targets in cancer therapy. *Nature reviews Cancer*. 2017;17(2):93–115.
16. Li KK, Ng IO, Fan ST, Albrecht JH, Yamashita K, Poon RY. Activation of cyclin-dependent kinases CDC2 and CDK2 in hepatocellular carcinoma. *Liver*. 2002;22(3):259–68.
17. Kim H, Lee MJ, Kim MR, Chung IP, Kim YM, Lee JY, Jang JJ: **Expression of cyclin D1, cyclin E, cdk4 and loss of heterozygosity of 8p, 13q, 17p in hepatocellular carcinoma: comparison study of childhood and adult hepatocellular carcinoma.** *Liver* 2000, **20**(2):173–178.
18. Che Y, Ye F, Xu R, Qing H, Wang X, Yin F, Cui M, Burstein D, Jiang B, Zhang DY. Co-expression of XIAP and cyclin D1 complex correlates with a poor prognosis in patients with hepatocellular carcinoma. *Am J Pathol*. 2012;180(5):1798–807.
19. Yamamoto H, Monden T, Ikeda K, Izawa H, Fukuda K, Fukunaga M, Tomita N, Shimano T, Shiozaki H, Monden M. Coexpression of cdk2/cdc2 and retinoblastoma gene products in colorectal cancer. *British journal of cancer*. 1995;71(6):1231–6.
20. Shi XN, Li H, Yao H, Liu X, Li L, Leung KS, Kung HF, Lu D, Wong MH, Lin MC. In Silico Identification and In Vitro and In Vivo Validation of Anti-Psychotic Drug Fluspirilene as a Potential CDK2 Inhibitor and a Candidate Anti-Cancer Drug. *PloS one*. 2015;10(7):e0132072.
21. Shi XN, Li H, Yao H, Liu X, Li L, Leung KS, Kung HF, Lin MC. Adapalene inhibits the activity of cyclin-dependent kinase 2 in colorectal carcinoma. *Mol Med Rep*. 2015;12(5):6501–8.
22. Shi X, Li H, Shi A, Yao H, Ke K, Dong C, Zhu Y, Qin Y, Ding Y, He YH, et al. Discovery of radoxanide as a dual CDK4/6 inhibitor for the treatment of skin cancer. *Oncol Rep*. 2018;40(3):1592–600.
23. Berman HM, Westbrook J, Feng Z, Gilliland G, Bhat TN, Weissig H, Shindyalov IN, Bourne PE. The Protein Data Bank. *Nucleic acids research*. 2000;28(1):235–42.
24. Huang Z, Wong CF. Inexpensive Method for Selecting Receptor Structures for Virtual Screening. *J Chem Inf Model*. 2016;56(1):21–34.
25. Irwin JJ, Shoichet BK. ZINC—a free database of commercially available compounds for virtual screening. *J Chem Inf Model*. 2005;45(1):177–82.
26. Irwin JJ, Sterling T, Mysinger MM, Bolstad ES, Coleman RG. ZINC: a free tool to discover chemistry for biology. *J Chem Inf Model*. 2012;52(7):1757–68.
27. Li H, Leung KS, Ballester PJ, Wong MH. istar: a web platform for large-scale protein-ligand docking. *PloS one*. 2014;9(1):e85678.
28. Li H, Leung KS, Wong MH. **idock: A multithreaded virtual screening tool for flexible ligand docking.** In: *2012 IEEE Symposium on Computational Intelligence in Bioinformatics and Computational Biology*

(CIBCB): 2012.

29. Wang S, Zhu Y, Zheng X. **Study and Application of Chou-Talalay Method for Anti-tumor Drug Combination.** *Chinese Journal of Modern Applied Pharmacy* 2013.
30. Ikeno A, Sumiya T, Minato H, Fujitani B, Masuda Y, Hosoki K, Kurono M, Yasuba M. Effects of monatepil maleate, a new Ca²⁺ channel antagonist with alpha₁-adrenoceptor antagonistic activity, on cholesterol absorption and catabolism in high cholesterol diet-fed rabbits. *Jpn J Pharmacol.* 1998;78(3):303–12.
31. Bull MS, Swindale S, Overend D, Hess EA. Suppression of *Boophilus microplus* populations with fluzaron—an acarine growth regulator. *Aust Vet J.* 1996;74(6):468–70.
32. Chin NX, Figueredo VM, Novelli A, Neu HC. In vitro activity of temafloxacin, a new difluoro quinolone antimicrobial agent. *European journal of clinical microbiology infectious diseases: official publication of the European Society of Clinical Microbiology.* 1988;7(1):58–63.
33. Van Nueten JM, Xhonneux R, Vanhoutte PM, Janssen PA. Vascular activity of ketanserin (R 41 468), a selective 5-HT₂ receptor antagonist. *Archives internationales de pharmacodynamie et de therapie.* 1981;250(2):328–9.
34. Donnelly LE, Rogers DF. Therapy for chronic obstructive pulmonary disease in the 21st century. *Drugs.* 2003;63(19):1973–98.
35. Sietnieks A. Involvement of 5-HT₂ receptors in the LSD- and L-5-HTP-induced suppression of lordotic behavior in the female rat. *J Neural Transm.* 1985;61(1–2):65–80.
36. Bramson HN, Hermann D, Batchelor KW, Lee FW, James MK, Frye SV: **Unique preclinical characteristics of GG745, a potent dual inhibitor of 5AR.** *The Journal of pharmacology and experimental therapeutics* 1997, **282**(3):1496–1502.
37. Danjou P, Molinier P, Berlin I, Patat A, Rosenzweig P, Morselli PL. Assessment of the anticholinergic effect of the new antihistamine mizolastine in healthy subjects. *Br J Clin Pharmacol.* 1992;34(4):328–31.
38. Nagase T, Ishiko J, Takaori S. [Effects of 1-[2-[bis(fluorophenyl)methoxy]ethyl]-4-(3-phenylpropyl) piperazine dihydrochloride (I-893) on turnover of dopamine and norepinephrine in the brain]. *Nihon yakurigaku zasshi Folia pharmacologica Japonica.* 1987;90(2):105–14.
39. Senderowicz AM. Flavopiridol: the first cyclin-dependent kinase inhibitor in human clinical trials. *Investig New Drugs.* 1999;17(3):313–20.
40. Kaur G, Stetler-Stevenson M, Sebers S, Worland P, Sedlacek H, Myers C, Czech J, Naik R, Sausville E. Growth inhibition with reversible cell cycle arrest of carcinoma cells by flavone L86-8275. *J Natl Cancer Inst.* 1992;84(22):1736–40.
41. Parry D, Guzi T, Shanahan F, Davis N, Prabhavalkar D, Wiswell D, Seghezzi W, Paruch K, Dwyer MP, Doll R, et al. Dinaciclib (SCH 727965), a novel and potent cyclin-dependent kinase inhibitor. *Mol Cancer Ther.* 2010;9(8):2344–53.
42. Gojo I, Sadowska M, Walker A, Feldman EJ, Iyer SP, Baer MR, Sausville EA, Lapidus RG, Zhang D, Zhu Y, et al. Clinical and laboratory studies of the novel cyclin-dependent kinase inhibitor dinaciclib (SCH 727965) in acute leukemias. *Cancer Chemother Pharmacol.* 2013;72(4):897–908.
43. Stephenson JJ, Nemunaitis J, Joy AA, Martin JC, Jou YM, Zhang D, Statkevich P, Yao SL, Zhu Y, Zhou H, et al. Randomized phase 2 study of the cyclin-dependent kinase inhibitor dinaciclib (MK-7965) versus

- erlotinib in patients with non-small cell lung cancer. *Lung cancer*. 2014;83(2):219–23.
44. Lao CD, Moon J, Fruehauf JP, Flaherty LE, Bury MJ, Ribas A, Sondak VK. **SWOG S0826: A phase II trial of SCH 727965 (NSC 747135) in patients with stage IV melanoma.** *Journal of Clinical Oncology* 2012.
45. Mita MM, Joy AA, Mita A, Sankhala K, Jou YM, Zhang D, Statkevich P, Zhu Y, Yao SL, Small K, et al. Randomized phase II trial of the cyclin-dependent kinase inhibitor dinaciclib (MK-7965) versus capecitabine in patients with advanced breast cancer. *Clin Breast Cancer*. 2014;14(3):169–76.
46. Kawana H, Tamaru J, Tanaka T, Hirai A, Saito Y, Kitagawa M, Mikata A, Harigaya K, Kuriyama T. Role of p27Kip1 and cyclin-dependent kinase 2 in the proliferation of non-small cell lung cancer. *Am J Pathol*. 1998;153(2):505–13.
47. Wikman H, Nymark P, Vayrynen A, Jarmalaite S, Kallioniemi A, Salmenkivi K, Vainio-Siukola K, Husgafvel-Pursiainen K, Knuutila S, Wolf M, et al: **CDK4 is a probable target gene in a novel amplicon at 12q13.3-q14.1 in lung cancer.** *Genes, chromosomes & cancer* 2005, **42**(2):193–199.
48. Weir BA, Woo MS, Getz G, Perner S, Ding L, Beroukhim R, Lin WM, Province MA, Kraja A, Johnson LA, et al. Characterizing the cancer genome in lung adenocarcinoma. *Nature*. 2007;450(7171):893–8.
49. Malumbres M, Barbacid M. Cell cycle, CDKs and cancer: a changing paradigm. *Nature reviews Cancer*. 2009;9(3):153–66.
50. Cobrinik D. Pocket proteins and cell cycle control. *Oncogene*. 2005;24(17):2796–809.
51. Meraldi P, Lukas J, Fry AM, Bartek J, Nigg EA. Centrosome duplication in mammalian somatic cells requires E2F and Cdk2-cyclin A. *Nat Cell Biol*. 1999;1(2):88–93.
52. Walker AJ, Wedam S, Amiri-Kordestani L, Bloomquist E, Tang S, Sridhara R, Chen W, Palmby TR, Fourie Zirkelbach J, Fu W, et al. FDA Approval of Palbociclib in Combination with Fulvestrant for the Treatment of Hormone Receptor-Positive, HER2-Negative Metastatic Breast Cancer. *Clinical cancer research: an official journal of the American Association for Cancer Research*. 2016;22(20):4968–72.
53. Lane EL, Cheetham S, Jenner P. Dopamine uptake inhibitor-induced rotation in 6-hydroxydopamine-lesioned rats involves both D1 and D2 receptors but is modulated through 5-hydroxytryptamine and noradrenaline receptors. *J Pharmacol Exp Ther*. 2005;312(3):1124–31.
54. Spealman RD, Madras BK, Bergman J. Effects of cocaine and related drugs in nonhuman primates. II. Stimulant effects on schedule-controlled behavior. *J Pharmacol Exp Ther*. 1989;251(1):142–9.
55. Howell LL, Byrd LD. Characterization of the effects of cocaine and GBR 12909, a dopamine uptake inhibitor, on behavior in the squirrel monkey. *J Pharmacol Exp Ther*. 1991;258(1):178–85.
56. Howell LL, Landrum AM. Effects of chronic caffeine administration on respiration and schedule-controlled behavior in rhesus monkeys. *J Pharmacol Exp Ther*. 1997;283(1):190–9.
57. Nagase T, Hotta K, Morita S, Sakai K, Yamane M, Omote M, Mizusawa H: **[Pharmacological effects of the novel dopamine uptake inhibitor 1-[2-[bis(4-fluorophenyl)-methoxy]ethyl]-4-(3-phenylpropyl) piperazine dihydrochloride (I-893) on the central nervous system].** *Nihon yakurigaku zasshi Folia pharmacologica Japonica* 1991, **98**(2):121–141.

Figures

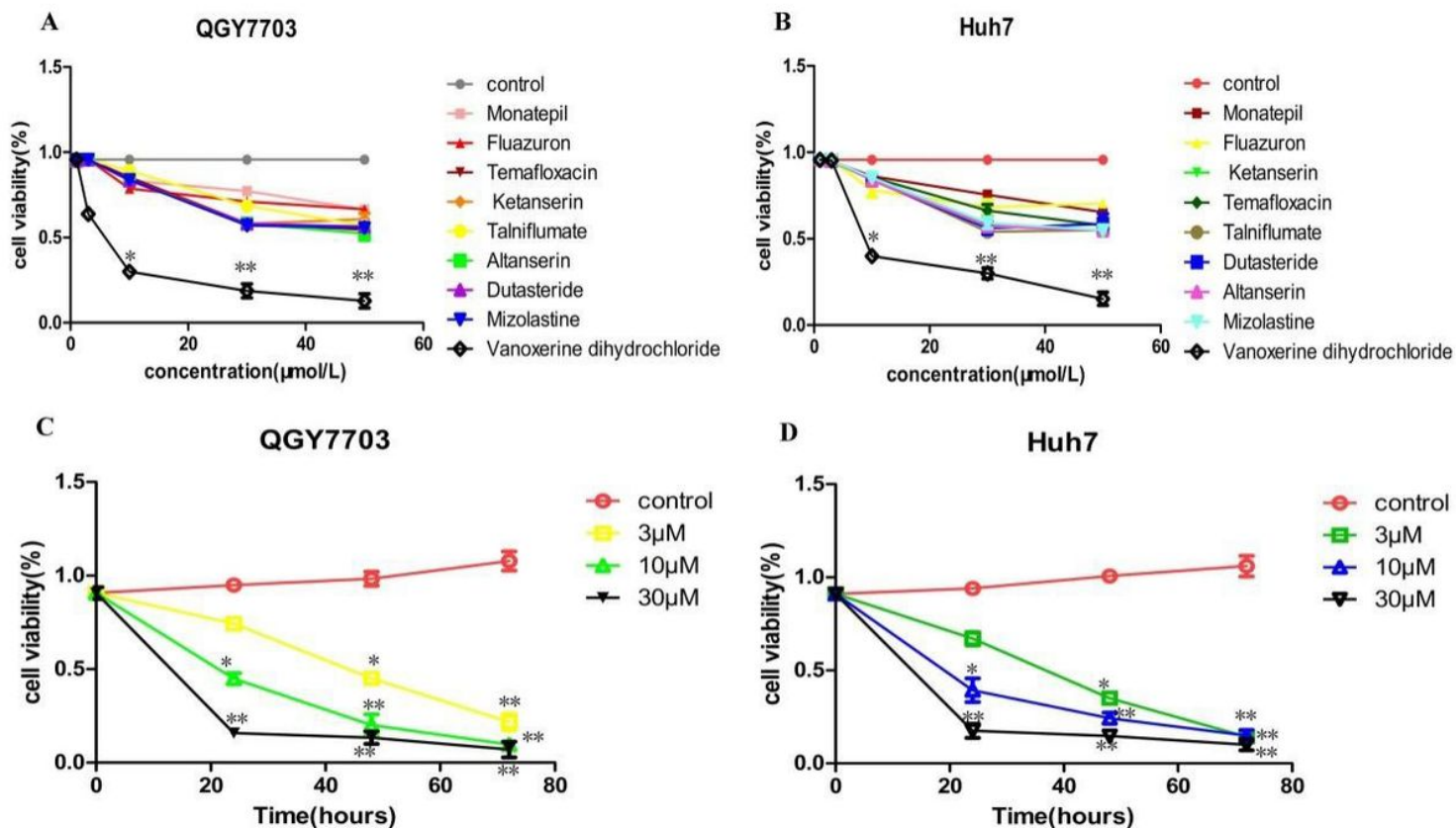


Figure 1

Figure 1

The effect of nine candidate CDK4/6 inhibitors on the viability of QGY7703 and Huh7 cells. The effect of nine candidate compounds on the cell viability of (A) QGY7703 and (B) Huh7 cell lines as determined by MTT assay. Vanoxerine dihydrochloride exhibited the highest cyto-toxicity in both cell lines. Vanoxerine dihydrochloride reduced cell viability dose- and time-dependently in(C) QGY7703 and (D) Huh7 cell lines. IC₅₀ values was calculated to be 3.79μM for QGY7703 and 4.04μM for Huh7. *p<0.05, significantly different from the control PBS treatment group.

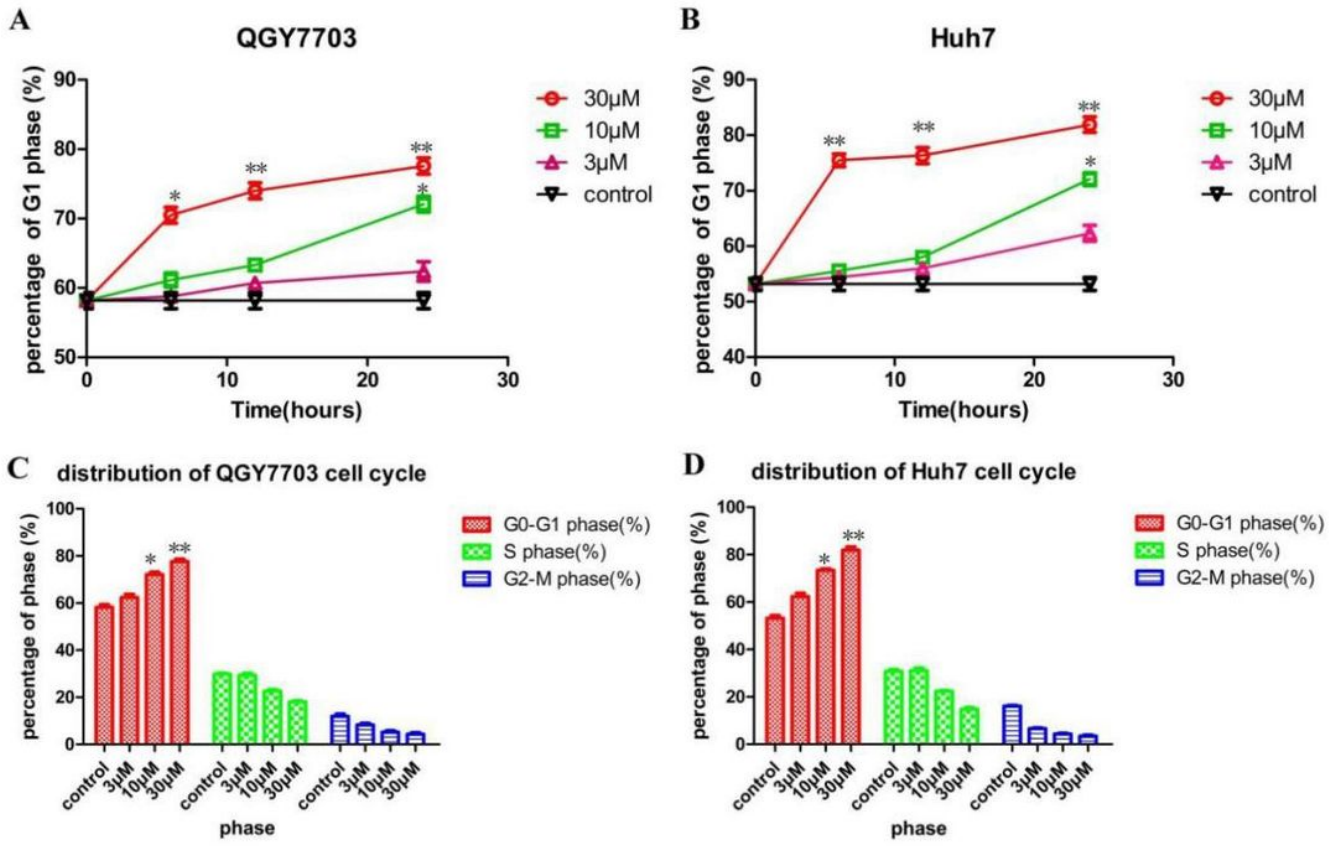


Figure 2

Figure 2

Effect of vanoxerine dihydrochloride treatment on cell cycle distribution in QGY7703 and Huh7 cells. (A) QGY7703 and (B) Huh7 cells were treated with different concentrations (3, 10 and 30μM) of vanoxerine dihydrochloride for 6, 12, 24hours. Cell cycle distributions were measured by flowcytometry. Vanoxerine dihydrochloride dose- and time-dependently increased the % of cells in G1 phase, as compared to PBS control. (B) The cell cycle distributions at 24 hours after 10μM vanoxerine dihydrochloride treatment. The bar graph indicated the percentage of the G1, S and G2-M phases. *p<0.05, significantly different from the control PBS treatment group.

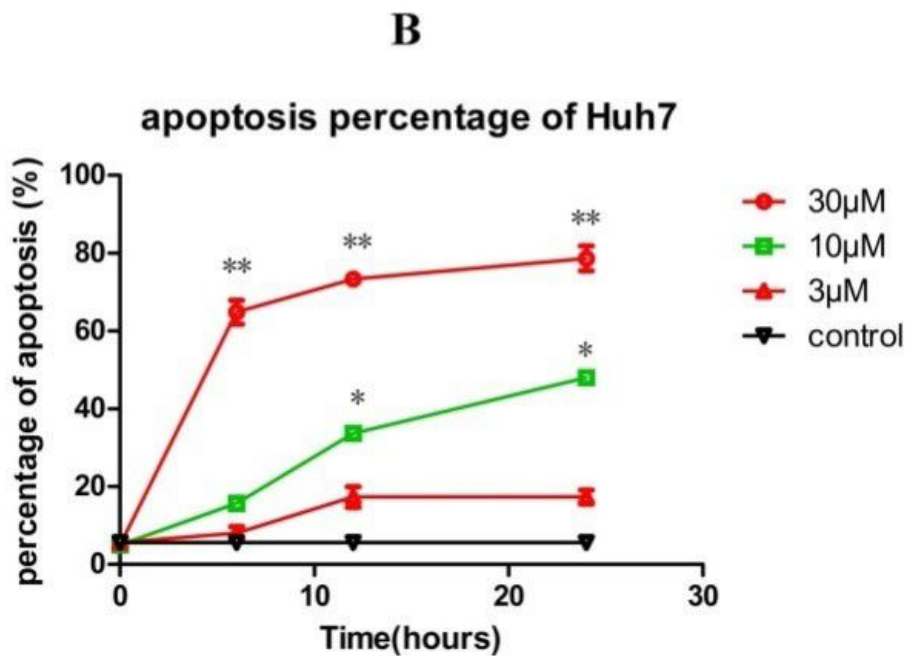
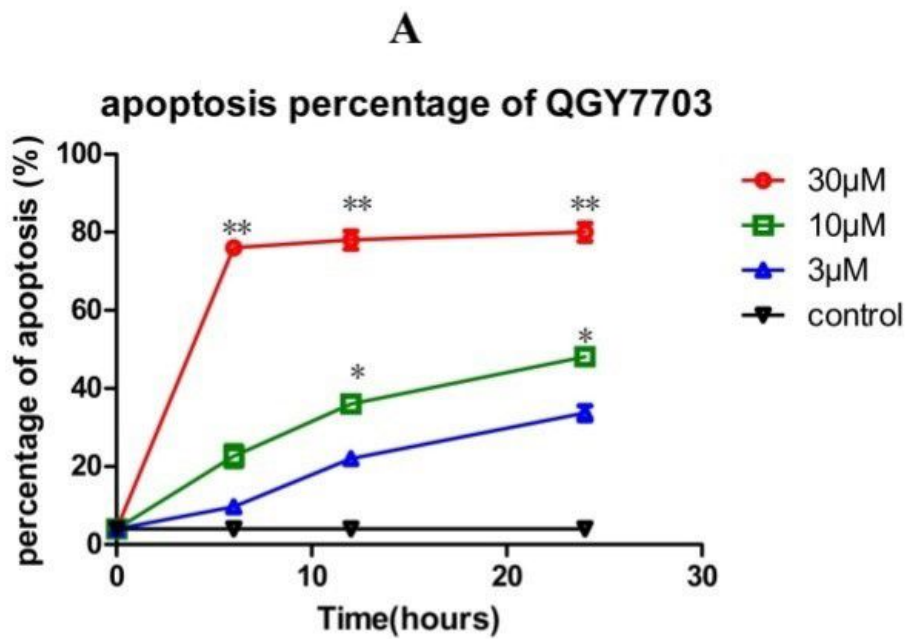


Figure 3

Figure 3

Vanoxerine dihydrochloride treatment induced cell apoptosis. Vanoxerine dihydrochloride treatment at 3, 10, 30µM concentration for 6, 12, 24h significantly increased the percentage of apoptosis in (A) QGY7703 and (B) Huh7 cell lines in a dose- and time-dependent manner. * $p < 0.05$, significantly different from the control PBS treatment group.

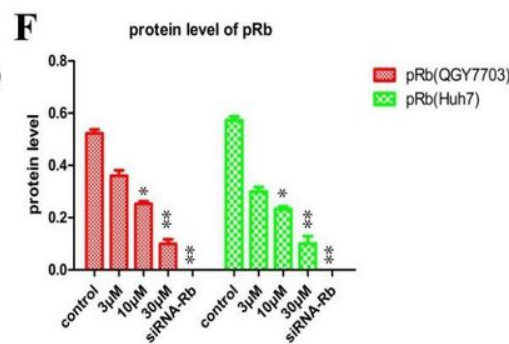
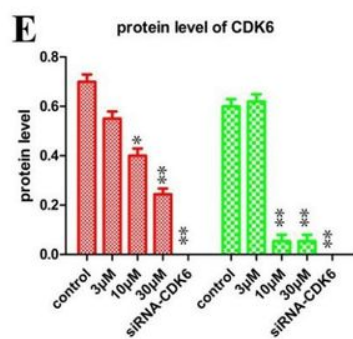
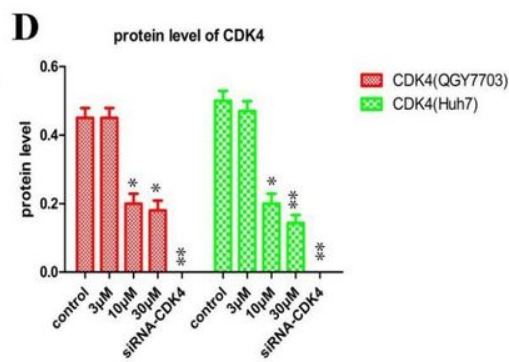
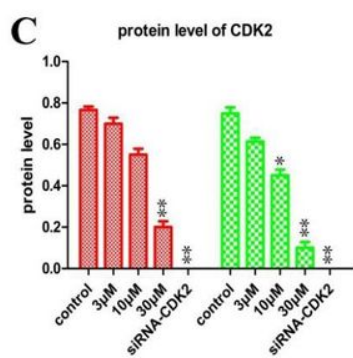
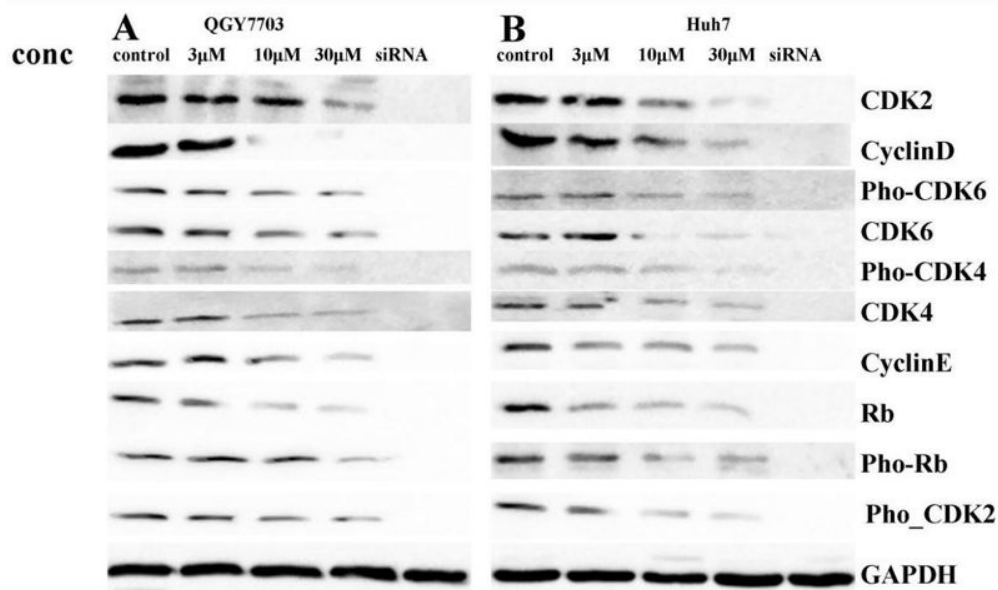


Figure 4

Figure 4

Effects of Vanoxerine dihydrochloride treatment on the expressions of proteins that play key roles in cell cycle progressions. (A) QHY7703 and (B) Huh7 cells were plated at 6-well plates with 0.125% FBS medium for 24 hours and then with 10%FBS medium containing various concentrations (3, 10, 30µM) of vanoxerine dihydrochloride. Cells were harvested after 6 hours incubation and proteins analyzed by Western blotting. Western blotting results showed that vanoxerine dihydrochloride treatment significantly reduced the expressions of CDK2/4/6, Rb, pho-CDK2/4/6, pho-Rb and cyclin D/E in QGY7703 and Huh7 cells. As positive

controls, three siRNAs targeting each of the CDK2/4/6 were designed as described previously[22], and used to inhibit the expressions of each of the CDK2/4/6 proteins. * $p < 0.05$, significantly different from the control PBS treatment group.

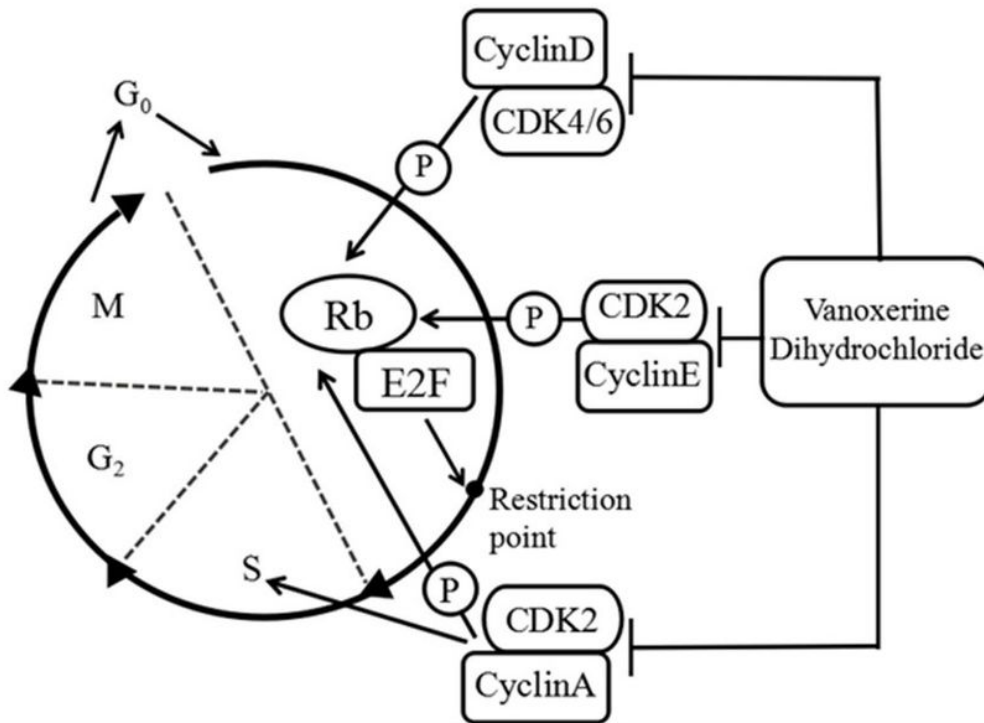


Figure 5

Figure 5

Mechanisms of vanoxerine dihydrochloride. Vanoxerine dihydrochloride inhibited CDK4/6 phosphorylation and the complex with cyclinD. It also inhibited CDK2 phosphorylation and the complex with cyclinE. Together, they suppress the hyperphosphorylation of RB, and the releases of pRB from its association with transcription factor E2F. As a result, it inhibits the cell cycle to proceed from G1 to S-phase. In addition, vanoxerine dihydrochloride also reduced cyclinA-CDK2 complex, and inhibited DNA replication and decrease S and G2-M phases.

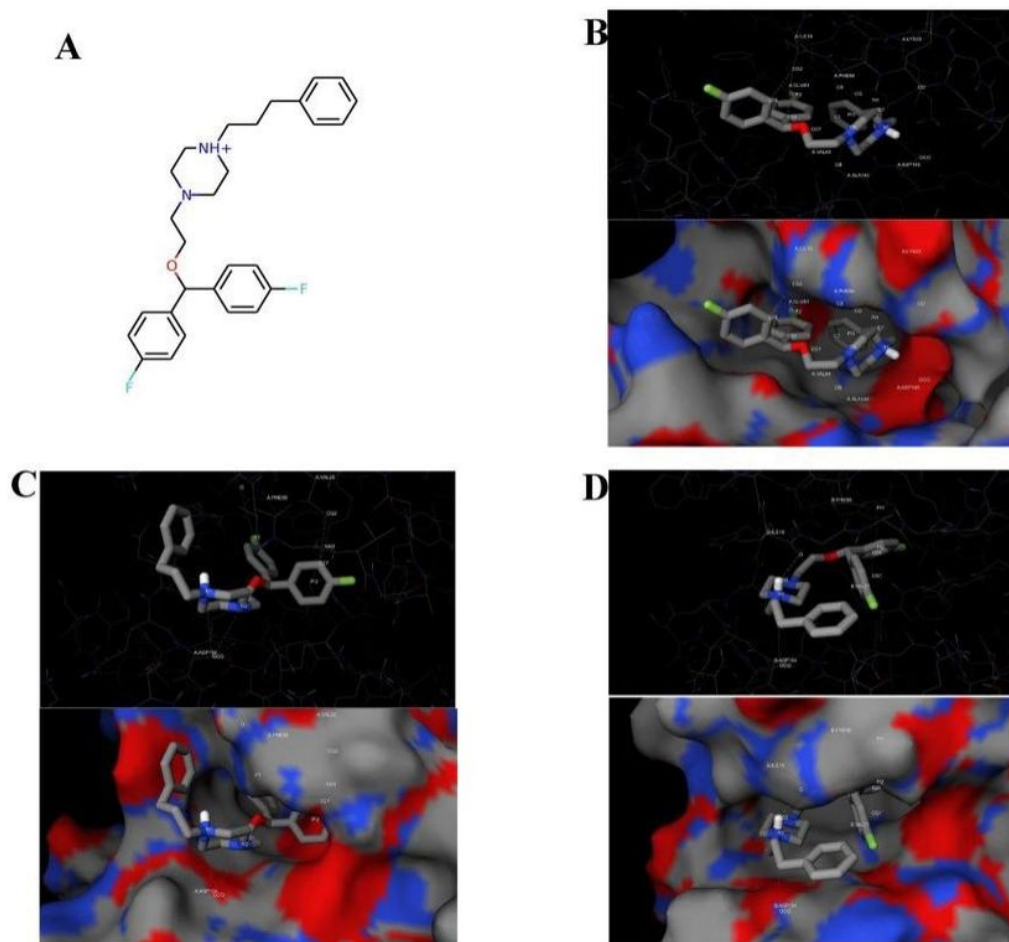


Figure 6

Figure 6

Structural analysis of the predicted conformation of vanoxerine dihydrochloride in CDK2/4/6 revealed critical binding interactions (A) The depicted two-dimensional structure of vanoxerine dihydrochloride. The predicted binding conformation in complex with (B) CDK2, (C) CDK4, and (D) CDK6. According to the docking result, vanoxerine dihydrochloride binds to CDK2 through hydrophobic contacts with ILE10, LYS33, VAL64, PHE80 and ALA144, a salt bridge with ASP145 and a halogen bond with GLU81. It interacts with CDK4 through two salt bridges with ASP104, a π interaction with LYS40, and a halogen bond with PHE98. It binds to CDK6 through a hydrogen bond with ILE19, a salt bridge with ASP104 and a π interaction with PHE98.

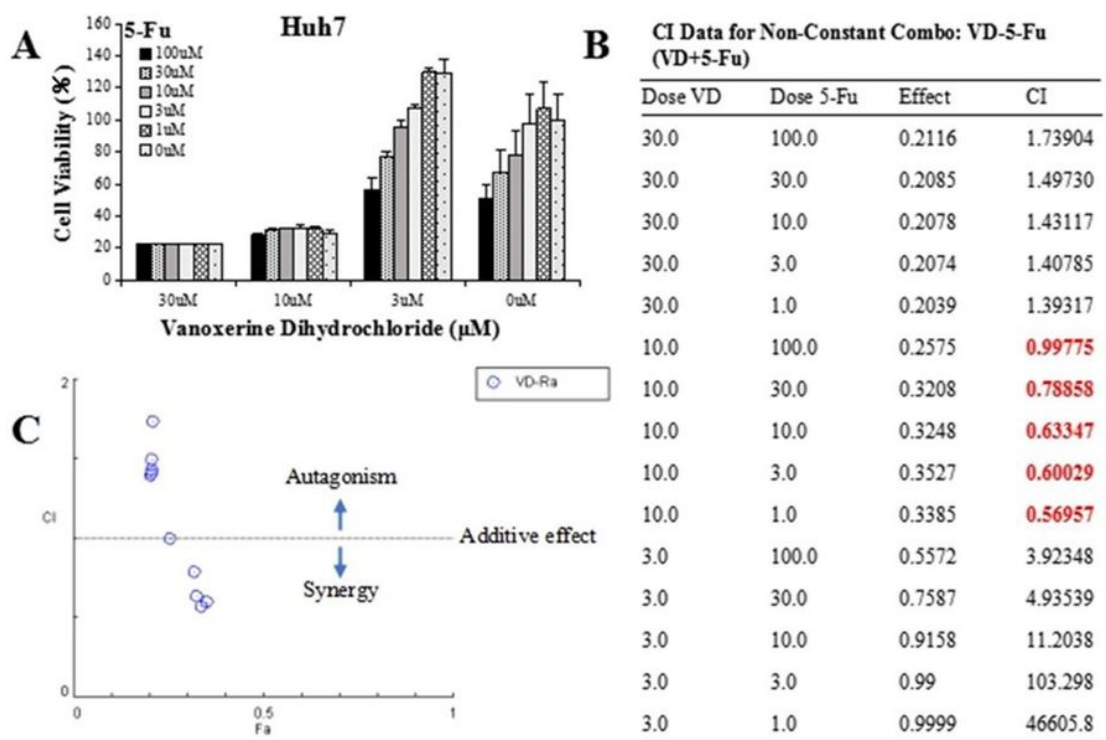


Figure 7

Figure 7

Combination of vanoxerine dihydrochloride and 5-FU produced synergistic cytotoxic effects in Huh7 cells. Huh7 cells were seeded in 96-well plates, and treated with indicated concentrations of vanoxerine dihydrochloride and 5-Fu. (A) Cell viability was detected by CCK8 after 72 hours treatment. (B) The combined effect was analyzed by CompuSyn software analysis of the Combination Index (CI) of the combined action. (C) A dot plot of the combined action of vanoxerine dihydrochloride and 5-Fu.

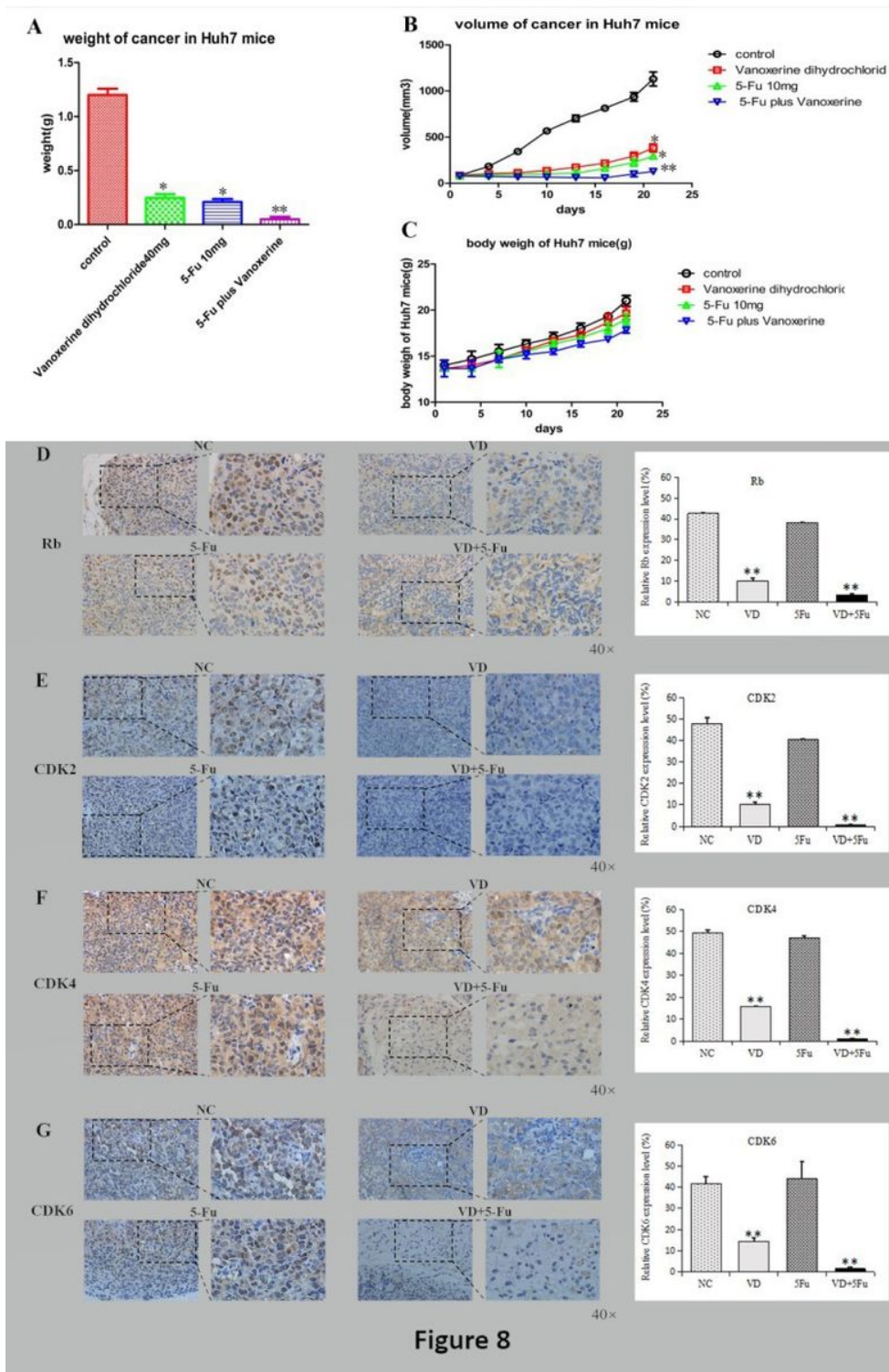


Figure 8

Vanoxerine dihydrochloride and 5-FU treatments reduced tumor growth in vivo in nude mice xenografted with Huh7 cells BALB/C nude mice xenografted with Huh7 cells were treated with vanoxerine dihydrochloride (40mg/kg), 5-Fu (10mg/kg), vanoxerine dihydrochloride (40mg/kg) plus 5-Fu (10mg/kg), and PBS for 21 days by daily i.p. injections. (A) Tumor volumes. (B) Tumor weight as compared to control at day 21 after treatment. (C) Body weight. (D-G) The representative pictures of immunohistochemistry staining of the

xenografted tumor tissues for (D) Rb, (E) CDK2, (F) CDK4, and (G) CDK6 expressions. ** $p < 0.01$, significantly different from the control PBS treatment group.